Adaptive Lower Bounds for Gaussian Measures of Polytopes

Uwe D. Hanebeck and **Maxim Dolgov**
Intelligent Sensor-Actuator-Systems Laboratory (ISAS)
Institute for Anthropomatics and Robotics
Karlsruhe Institute of Technology (KIT), Germany
Uwe.Hanebeck@kit.edu, Maxim.Dolgov@kit.edu

***Abstract*—In this paper, we address the problem of probability mass computation of a multivariate Gaussian contained within a polytope. This computation requires an evaluation of a multivariate definite integral of the Gaussian, whose solution is not tractable for higher dimensions in a reasonable amount of time. Thus, research concentrates on the derivation of approximate but sufficiently fast computation methods. We propose a novel approach that approximates the underlying integration domain, namely the polytope, using disjoint sectors such that the probability mass contained within the sectors is maximized. In order to derive our main algorithm, we first propose an approach to approximate volume computation of a polytope using disjoint sectors. This solution is then extended to the computation of the probability mass of a Gaussian contained within the polytope. The presented solution provides a lower bound on the true probability mass contained within the polytope. Because the initial optimization problem is highly nonlinear, we propose a greedy algorithm that splits the sectors with the highest probability mass.**

Keywords*—*Polytope volume, nonlinear optimization, chance constraints, spherical coordinates.

I. Introduction

Many practical application such as optimization with chance constraints [1], [2], [3], chance-constrained control [4], [5], [6], or evaluation of the non-centered orthant probability [7], i.e., the probability that all elements of a random vector have positive coordinates, require computation of the probability mass of a multivariate Gaussian probability density function (pdf) over a compact domain. Numerical evaluation of the corresponding integral is usually computationally intense [8], [9]. Thus, it is not suitable for real-time applications because the computation of the probability mass is often embedded into an iterative optimization procedure, which requires the evaluation of the integral at each iteration step. Therefore, research concentrates on development of approximate but fast integration methods.

One of the simplest approximation methods is to compute the largest ellipsoid that fits into the polytope. The position and the orientation of this ellipsoid are determined by the position and the covariance of the Gaussian. This method and its application to chance-constrained control of linear stochastic systems was presented, e.g., in [10], [11]. The main advantage of this method is that it is extremely fast. However, it is very conservative, i.e., the computed lower bound on the real probability mass contained within the polytope is not tight.

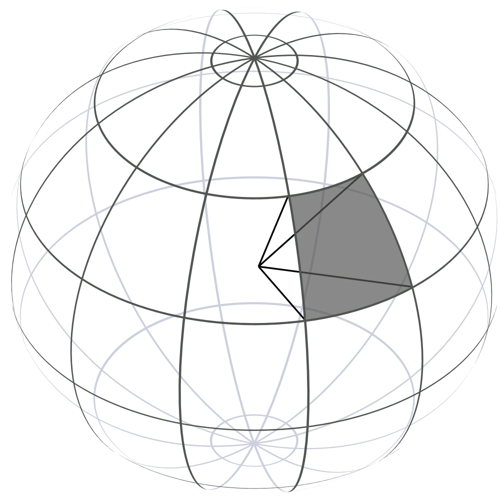

Figure 1: Sector of a 3D-sphere [12].

Another conservative approximation method consists in the application of Boole's inequality. Using this inequality, it is possible to separate the polytopic integration domain into multiple integrations over individual half spaces determined by the linear constraints that define the polytope [1], [2], [13].

In contrast to deterministic conservative approximations, methods based on random sampling approximate the Gaussian using samples also referred to as particles. By doing so, the evaluation of the integral of the Gaussian over the polytopic domain reduces to the summation of the weights of the samples that fall into the polytope [3], [14]. However, because the sampling is random, the approximation is also non-deterministic. An important contribution was made in [15] and [16] by deriving the required number of samples in order to provide a specified confidence level.

The contributions of this paper are the following. We propose a new method to compute a lower bound on the probability mass of a multivariate Gaussian over a polytopic domain. The tightness of the bound is a design parameter that can be traded for computation time. Obtaining a lower bound is of interest for, e.g., chance-constrained control and optimization. However, with minor modifications, the proposed approach can also be used to compute an upper bound on the true result. This modification can be used in order to define a stopping criterion for our algorithm that yields tight bounds. In contrast to available methods that approximate the probability density, our approach approximates the domain, namely the polytope. Before addressing this problem, we first derive an algorithm to approximate the polytope from the inside using disjoint n-spherical sectors. This method is then extended to computation of the probability mass of the standard Gaussian contained within the polytope. To approximate the probability mass of arbitrary Gaussians, we propose to convert them into standard Gaussian using a linear transformation and to apply the presented algorithm afterwards. The derived algorithm converts the numerical integration problem into an optimization problem. Thus, it can be solved using standard optimization algorithms.

Outline. The paper is organized as follows. In the next section, we formulate the considered problem. Before solving this problem, we first address the inner approximation of a polytope using disjoint sectors in Sec. III. Results from Sec. III are extended to the computation of the probability mass of a Gaussian in Sec. IV. A numerical example is presented in Sec. V and Sec. VI concludes the paper.

Notation. In this paper, we use the following notation. Vector-valued quantities are underlined ($\underline{x}$), while matrices are in bold capital letters ($\mathbf{A}$). Random variables are in bold letters $\boldsymbol{a}, \underline{\boldsymbol{x}}$. The notation $\boldsymbol{x} \sim f(x)$ denotes that the random variable $\boldsymbol{x}$ is distributed according to the probability density function (pdf) $f(\cdot)$. The identity matrix is denoted by $\mathbf{I}$ and the zero-vector by $\underline{0}$. We abbreviate the sequences $a_1, a_2, \ldots, a_n$ as $a_{1:n}$.

II. Problem Formulation

We consider the following problem. Given a multivariate Gaussian $\mathcal{N}\left(\underline{\mu}, \mathbf{C}\right)$ with pdf defined according to

$$f(\underline{\boldsymbol{x}}) = \frac{1}{(2\pi \det(\mathbf{C}))^{\frac{n}{2}}} \exp\left(-\frac{1}{2}(\underline{\boldsymbol{x}} - \underline{\mu})^\top \mathbf{C}^{-1}(\underline{\boldsymbol{x}} - \underline{\mu})\right)$$

with mean $\underline{\mu} \in \mathbb{R}^n$ and positive definite covariance matrix $\mathbf{C} \in \mathbb{R}^{n \times n}$, $n \in \mathbb{N}$, we seek to compute the probability mass of $\mathcal{N}\left(\underline{\mu}, \mathbf{C}\right)$ contained within a given polytope $\mathcal{P}$, i.e., the probability

$$\mathrm{P}(\underline{\boldsymbol{x}} \in \mathcal{P}) = \int_{\underline{x} \in \mathcal{P}} f(\underline{x}) \, \mathrm{d}\underline{x} \qquad (1)$$

that a sample $\underline{x}$ of the random variable $\underline{\boldsymbol{x}} \sim \mathcal{N}\left(\underline{\mu}, \mathbf{C}\right)$ lies within the polytope $\mathcal{P}$. The polytope is given either as a set of vertices $\mathcal{V}$ or in terms of linear constraints

$$\mathcal{P} = \{\underline{x} \in \mathbb{R}^n : \mathbf{A}\underline{x} \leq \underline{b}\} \ ,$$

where $\mathbf{A} \in \mathbb{R}^{m \times n}$ and $\underline{b} \in \mathbb{R}^m$, $m \in \mathbb{N}$. The interior of the polytope $\mathcal{P}$ is not empty. We will assume that the polytope is represented in terms of linear constraints. The representation in terms of vertices can be converted into the latter by computing the convex hull of the vertices. Furthermore, the following assumption is required to hold.

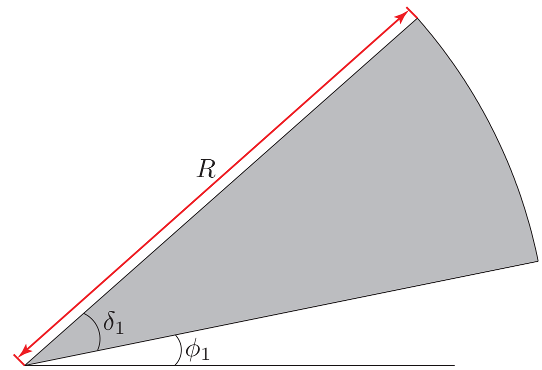

Figure 2: Two-dimensional illustration of the vector $\underline{\xi}$ (see (2)) that defines a sector.

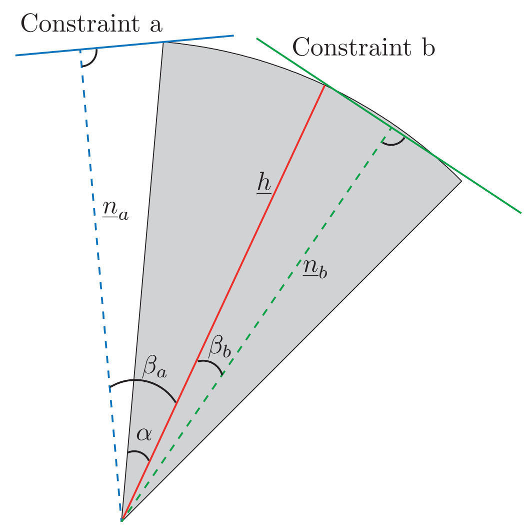

Figure 3: Two-dimensional illustration of the sector arc satisfying and violating linear constraints $\mathbf{A}\underline{x} \leq \underline{b}$.

Assumption 1: The mean of the considered Gaussian $\mathcal{N}\left(\underline{\mu}, \mathbf{C}\right)$ is contained within the polytope $\mathcal{P}$, i.e., it holds $\mathbf{A}\underline{\mu} \leq \underline{b}$.

Because an exact evaluation of (1) is computationally intense, we will derive an algorithm that computes the lower bound

$$\widetilde{\mathrm{P}}\left(\underline{\boldsymbol{x}} \in \mathcal{P}\right) \leq \mathrm{P}(\underline{\boldsymbol{x}} \in \mathcal{P})$$

in the remainder of the paper. At this point, we also note that it is sufficient to consider the standard Gaussian $\mathcal{N}\left(\underline{0}, \mathbf{I}\right)$ because introducing the substitution

$$\underline{\boldsymbol{z}} = \mathbf{T}^{-1}\left(\underline{\boldsymbol{x}} - \underline{\mu}\right) \ ,$$

where $\mathbf{T} = \mathbf{C}^{\frac{1}{2}}$ is the Cholesky decomposition of $\mathbf{C}$, we can convert every Gaussian into the standard Gaussian. Application of this transformation to $\mathcal{P}$ yields the transformed polytope

$$\mathcal{P}^* = \{\underline{x} : \mathbf{AT}\underline{x} \leq \underline{b} - \mathbf{A}\underline{\mu}\} \ .$$

III. Sector-based Approximation of Polytopes

In this section, we describe an approach to approximate volume computation of the polytope $\mathcal{P}$ using disjoint sectors that are fitted into the polytope from the inside. For the three-dimensional case such a sector is depicted in Fig. 1. The sectors are determined by the following vector

$$\underline{\xi}_i = [R \quad \phi_1 \quad \phi_2 \quad \dots \quad \phi_{n-1} \quad \delta_1 \quad \delta_2 \quad \dots \quad \delta_{n-1}] \ , \quad (2)$$

where $[R \quad \phi_1 \quad \phi_2 \quad \dots \quad \phi_{n-1}]$ are the n-spherical coordinates (see Appendix A) of the main sector axis with $R > 0$, $\phi_{1:n-2} \in [0;\pi)$, $\phi_{n-1} \in [0;2\pi)$, and $[\delta_1 \quad \delta_2 \quad \dots \quad \delta_{n-1}]$ are the opening angles that correspond to $\phi_{1:n-1}$ with $\delta_{1:n-2} \in [0;\pi)$, $\delta_{n-1} \in [0;2\pi)$. Fig. 2 shows the components of $\underline{\xi}$ in 2D.

The point from which the sectors originate must lie within the polytope. We assume the origin to be this point. If this is not the case, perform the coordinate transform

$$\underline{z} = \underline{x} - \underline{\hat{y}} \ ,$$

where $\underline{\hat{y}}$ is an arbitrary interior point of the polytope, i.e., it holds $\mathbf{A}\underline{\hat{y}} \leq \underline{b}$.

The approximation of the polytope is performed such that the volume V contained within the sectors is maximized under the constraints that each sector is contained within the polytope and that the sectors do not overlap. This optimization problem for a fixed number of sectors $s \in \mathbb{N}_+$ is formalized in Problem 1.

Problem 1: The inner sector approximation of the non-empty polytope $\mathcal{P} = \{\underline{x} : \mathbf{A}\underline{x} \leq \underline{b}\}$, with $\mathbf{A} \in \mathbb{R}^{m \times n}$ and $\underline{b} \in \mathbb{R}^m$, $m \in \mathbb{N}$ that contains the origin, i.e., $\underline{0} \leq \underline{b}$, with $s \in \mathbb{N}_+$ disjoint sectors is the solution of the optimization problem

$$\begin{aligned} \max_{\underline{\xi}_i} \quad & \sum_{i=1}^{s} V_i \\ \text{s.t.} \quad & \mathcal{S}_i \in \mathcal{P} \ , \forall i \ , \\ & \mathcal{S}_i \cap \mathcal{S}_j = \varnothing, \text{for } i \neq j \ \forall i,j \ , \\ & \xi_{i,1} > 0 \ , \ \xi_{i,2:n-1} \in [0;\pi) \ , \ \xi_{i,n} \in [0;2\pi) \ \forall i \ , \\ & \xi_{i,n+1:2n-2} \in [0;\pi), \ \xi_{i,2n-1} \in [0;2\pi) \ \forall i \ , \end{aligned} \quad (3)$$

where V_i denotes the volume contained within sector $\mathcal{S}_i$.

The formula for the volume V_i is given in the following theorem.

Theorem 1: The volume of a single sector $\mathcal{S}_i$ is given by

$$V_i = \frac{1}{n} R^n \delta_{n-1} \prod_{i=1}^{n-2} \left[\gamma_i(\delta_{n-i-1}) - \gamma_i(0)\right] \ , \quad (4)$$

where for even n, $\gamma_n(\alpha)$ is defined according to

$$\gamma_n(\alpha) = \alpha \prod_{j=0}^{\frac{n-2}{2}} \frac{n-2j-1}{n-2j} + \sum_{i=0}^{\frac{n-2}{2}} \prod_{j=0}^{i-1} \frac{n-2j-1}{n-2j} \left(-\frac{1}{n-2i}\right) \sin^{n-2i-1}(\alpha)\cos(\alpha) \ ,$$

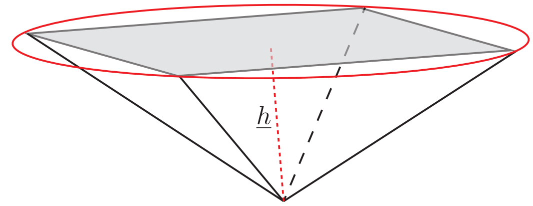

Figure 4: Ellipsis that specifies the opening angle for evaluation of constraint violation by the sector arc.

and for odd n according to

$$\gamma_n(\alpha) = \sum_{i=0}^{\frac{n-1}{2}} \prod_{j=0}^{i-1} \frac{n-2j-1}{n-2j} \left(-\frac{1}{n-2i}\right) \sin^{n-2i-1}(\alpha)\cos(\alpha) \, .$$

Proof: The proof is given in Appendix B. ■

In what follows, we discuss how to check the constraints in (3).

In order to check, if the sector $\mathcal{S}_i$ is inside the polytope, we propose a two-level approach. In the first step, we check if the sector vertices $\underline{v}_{i,j}$ for $j = 1, \dots, 2^n$ in Cartesian coordinates satisfy

$$\mathbf{A}\underline{v}_{i,j} \leq \underline{b} \ . \quad (5)$$

For an n-dimensional sector, the vertices can be calculated according to

$$\underline{v}_{i,j} = [R_i \quad \phi_{i,1} \quad \dots \quad \phi_{i,n-1}] + [0 \quad c_1\delta_1 \quad \dots \quad c_{n-1}\delta_{n-1}] \ ,$$

where all 2^n combinations of $c_j \in \{0,1\}$ are considered. The conversion from spherical into Cartesian coordinates can be performed according to Appendix A.

If any of the vertices $\underline{v}_{i,j}$ does not satisfy (5), the sector is not inside the polytope. On the other hand, if the vertices are within the polytope, we need to check if the sector arc is also inside the polytope. To illustrate this issue, consider the two-dimensional scenario depicted in Fig. 3. In this figure, it can be seen that the arc satisfies the constraint a and does not satisfy the constraint b. Constraint a is satisfied because the angle β_a between the normal of the constraint and the central sector axis $\underline{h}$ with

$$\underline{h} = \left[R_i \quad \phi_{i,1} + \tfrac{\delta_{i,1}}{2} \quad \phi_{i,2} + \tfrac{\delta_{i,2}}{2} \quad \dots \quad \phi_{i,n-1} + \tfrac{\delta_{i,n-1}}{2}\right]$$

is larger than the opening angle α. However, this is not the case for constraint b. Generalization of this scenario to higher dimensions is depicted in Fig. 4. In these dimensions, the opening angle α is specified by an ellipsoid through the sector vertices. Because direct evaluation is difficult, we propose to transform the ellipsoid into a hypersphere. This transformation is given by

$$\mathbf{M} = \left(\mathbf{R}^{\frac{1}{2}}\right)^{-1} \ ,$$

where $\mathbf{R}$ is the empirical covariance of the sector vertices with

$$\mathbf{R} = \frac{1}{2^n} \sum_{i=1}^{2^n} \left(\underline{v}_i - \underline{h}\right)\left(\underline{v}_i - \underline{h}\right)^\top \ .$$

Its square root can be obtained using the Cholesky decomposition. If we apply the described transformation, we only have to guarantee that the angle between the transformed central axis $\underline{\widetilde{h}}$ and any of the transformed vertices $\underline{\widetilde{v}}_{i,j}$ remains larger than the angle between $\underline{\widetilde{h}}$ and the transformed normal $\underline{\widetilde{n}}$ of the considered constraint in order to satisfy the constraint that the sector arc must be inside the polytope.

To guarantee that the sectors are disjoint, i.e., that $\mathcal{S}_i \cap \mathcal{S}_j = \varnothing$, for $i \neq j$ holds, we propose to check if any of the vertices of sector $\mathcal{S}_i$ lies within the pyramid with infinite height determined by the origin and the vertices of sector $\mathcal{S}_j$.

Problem 1 has two significant disadvantages: (i) the number of sectors is fixed a priori and (ii) the optimization problem is highly nonlinear. Thus, we propose to implement the sector approximation as a greedy algorithm given in Algorithm 1.

Algorithm 1: Greedy sector approximation.

Input: Constraints $\mathbf{A}, \underline{b}$, termination condition ϵ
Output: List of sectors $\mathcal{S}$

```
S = ∅;
S_1 ← largest n-sphere that fits into the polytope;
S ← S ∪ S_1;
while NOT ε do
    j ← arg max_j V_j;
    S ← S \ S_j;
    S_{j,1}, S_{j,2} ← Split S_j;
    S ← S ∪ {S_{j,1}, S_{j,2}};
end
```

Remark 1: There are many different possibilities how to design the termination condition ϵ in Algorithm 1. The simplest one is to fix the number of sectors that approximate the polytope. This condition is directly related to the number of splits and recovers the initial optimization problem (3). Another possible termination condition is to fix the minimum difference between the volume contained within the sectors before splitting and after the splitting.

The main step of the greedy procedure described in Algorithm 1 is the splitting of the sector with the largest volume into two new sectors. Splitting into more than two new sectors is possible and the generalization to this case is trivial. As the initial guesses, we use $\mathcal{S}_{i,1}$ with

$$
\begin{aligned}
\underline{\xi}_{i,1} = [R_i \quad & \phi_{i,1} + e_1\delta_{i,1} \quad \dots \quad \phi_{i,n-1} + e_{n-1}\delta_{i,n-1} \\
& (1-e_1)\delta_1 \quad \dots \quad (1-e_{n-1})\delta_{n-1}] \ ,
\end{aligned}
$$

and $\mathcal{S}_{i,2}$ with

$$
\begin{aligned}
\underline{\xi}_{i,2} = [R_i \quad & \phi_{i,1} \quad \dots \quad \phi_{i,n-1} \\
& (1-e_1)\delta_1 \quad \dots \quad (1-e_{n-1})\delta_{n-1}] \ ,
\end{aligned}
$$

where $\underline{e}$ is a vector with one element being 0.5 and all others being 0. The element $e_j = 0.5$ of $\underline{e}$ specifies in which direction we split the initial vector. In our current implementation, we choose $\underline{e}$ randomly. Another possibility is to split in the direction of the largest sector extension. The splitting procedure is given in Algorithm 2.

Algorithm 2: Sector splitting.

Input: Sector $\mathcal{S}_i$, $\mathcal{S} \setminus \mathcal{S}_i$, constraints $\mathbf{A}, \underline{b}$
Output: Sectors $\mathcal{S}_{i,1}$ and $\mathcal{S}_{i,2}$

Set initial guesses to $\mathcal{S}_{i,1}$ and $\mathcal{S}_{i,2}$;
Add constraint $\mathcal{S}_{i,j} \cap \{\mathcal{S} \setminus \mathcal{S}_i\} = \varnothing, j \in \{1,2\}$ to (3);
Solve the modified version of (3) for s=2;

Remark 2: It can happen that the new sectors do not expand into non-covered regions of the polytope in the direction where the sector $\mathcal{S}_i$ already touches the constraints. Thus, we suggest to slightly reduce the radii of the initial guesses $\mathcal{S}_{i,1}$ and $\mathcal{S}_{i,2}$. Simulations indicate that a reduction by 20% usually suffices.

Having derived the sector approximation method, we generalize it to the computation of the probability mass within a polytope in the next section.

IV. Sector-Based Probability Mass Approximation

In what follows, we first address the approximation of the probability mass of a standard Gaussian $\mathcal{N}(\underline{0}, \mathbf{I})$ contained in a polytope. To compute this probability mass, we extend the inner sector approximation derived in Sec. III from the approximation that maximizes the volume to approximation that maximizes the probability mass contained within the sectors. This maximization is performed under the constraints that each sector is contained within the polytope and that the sectors do not overlap. Problem 2 formalizes the described optimization problem.

Problem 2: The conservative approximation of the probability mass of the standard Gaussian $\mathcal{N}(0, \mathbf{I})$ contained within the non-empty polytope $\mathcal{P} = \{\underline{x} : \mathbf{A}\underline{x} \le \underline{b}\}$, where $\mathbf{A} \in \mathbb{R}^{m \times n}$ and $\underline{b} \in \mathbb{R}^m$, $m \in \mathbb{N}$ that contains the origin, i.e., $\underline{0} \le \underline{b}$, using s, $s \in \mathbb{N}+$ disjoint sectors is the solution of the optimization problem

$$
\begin{aligned}
\max_{\underline{\xi}_i} \quad & \sum_{i=1}^{s} \mathrm{P}(x \in \mathcal{S}_i) \\
\text{s.t.} \quad & \mathcal{S}_i \in \mathcal{P} \ , \forall i \ , \\
& \mathcal{S}_i \cap \mathcal{S}_j = \varnothing, \text{for } i \neq j \ \forall i, j \ , \\
& \xi_{i,1} > 0 \ , \ \xi_{i,2:n-1} \in [0;\pi) \ , \ \xi_{i,n} \in [0;2\pi) \ \forall i \ , \\
& \xi_{i,n+1:2n-2} \in [0;\pi), \ \xi_{i,2n-1} \in [0;2\pi) \ \forall i \ .
\end{aligned} \tag{6}
$$

The probability mass $\mathrm{P}(x \in \mathcal{S}_i)$ is given in Theorem 2.

Theorem 2: The probability mass of a standard Gaussian $\mathcal{N}(\underline{0}, \mathbf{I})$ contained within a single sector $\mathcal{S}_i$ is given by

$$
\begin{aligned}
\mathrm{P}(\underline{x} \in \mathcal{S}_i) = & \frac{1}{2\pi^{\frac{n}{2}}} \delta_{n-1} \prod_{i=1}^{n-2} \left[\gamma_i(\delta_{n-i-1}) - \gamma_i(0)\right] \\
& \times \left[\Gamma\left(\frac{n}{2}\right) - \Gamma\left(\frac{n}{2}, \frac{R^2}{2}\right)\right] \ ,
\end{aligned} \tag{7}
$$

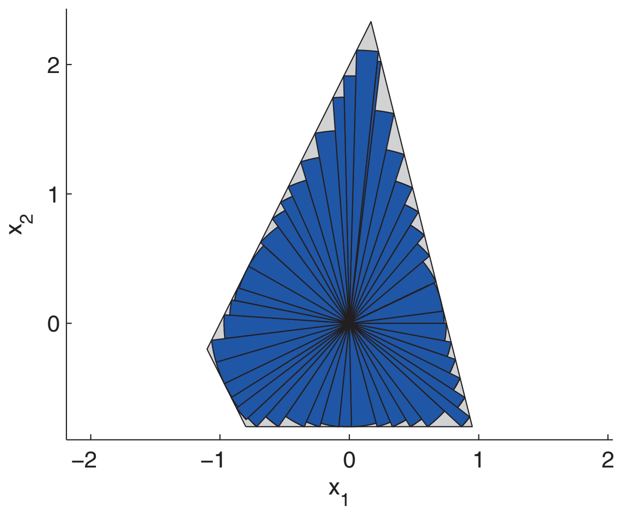

(a) Polytope $\mathcal{P}_1$.

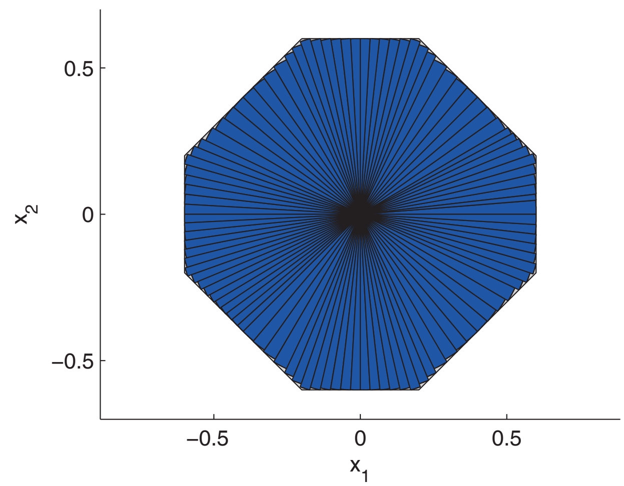

(b) Polytope $\mathcal{P}_2$.

Figure 5: Visualization of the approximation of $\mathcal{P}_1$ and $\mathcal{P}_2$ after 100 splittings.

where $\Gamma(\cdot)$ is the Gamma function and $\Gamma(\cdot,\cdot)$ is the incomplete Gamma function

$$\Gamma(x,y) = \int_y^\infty t^{x-1} \exp(-t) \, \mathrm{d}t \ .$$

Proof: In order to calculate the probability mass contained within the sector $\mathcal{S}_i$, we need to evaluate the following integral

$$\mathrm{P}(\underline{x} \in \mathcal{S}_i) = \frac{1}{(2\pi)^{\frac{n}{2}}} \int_0^R \int_0^{\delta_1} \cdots \int_0^{\delta_{n-1}} \exp\left(-\frac{r^2}{2}\right) \mathrm{d}V \ ,$$

where we exploited the spherical symmetry of the standard Gaussian by changing the angular integration interval from $[\phi_j; \phi_j + \delta_j]$ to $[0; \delta_j]$, $j = 1, \dots, n-1$. Because the sectors are axis-aligned, we can calculate the integrals w.r.t. the individual variables independently. For the integration w.r.t. the radius, it holds [17]

$$\int_0^R r^{n-1} \exp\left(-\frac{r}{2}\right) \mathrm{d}r = 2^{\frac{n-2}{2}} \left(\Gamma\left(\frac{n}{2}\right) - \Gamma\left(\frac{n}{2}, \frac{R^2}{2}\right) \right) \ .$$

Integration w.r.t. the angles $\phi_{1:n-1}$ is performed according to the proof of Theorem 1. Combining the individual results concludes the proof. ■

In order to compute the probability mass of the standard Gaussian contained within the polytope $\mathcal{P}$, we can use Algorithms 1 and 2 with the following modifications.

1) In Algorithm 1, replace the computation of the sector with the highest volume ($j \leftarrow \arg\min_j V_j$) by $j \leftarrow \arg\max_j \mathrm{P}(\underline{x} \in \mathcal{S}_j)$.
2) In Algorithm 2, modify problem (6) instead of (3).

Remark 3: The provided algorithm approximates the polytope with disjoint sectors from the inside. It is possible to derive an algorithm that approximates the polytope from the outside. For this purpose, it is necessary to replace the constraint in Algorithm 1 that the sectors must be within the polytope by the constraint that the polytope must be within the sectors. Furthermore, the volume (probability mass) contained within the sectors must be minimized. With these changes, it is possible to design a stopping criterion for Algorithm 1 that is based on the difference between the volume (probability mass) computed using the inner and the outer approximation.

In the next section, we provide a numerical example of the proposed probability mass computation algorithm.

V. Numerical Example

To demonstrate the presented algorithm, we compute the probability mass of the standard Gaussian $\mathcal{N}(\underline{0}, \mathbf{I})$ within the polytopes $\mathcal{P}_1$ and $\mathcal{P}_2$ with

$$\mathbf{A}_1 = \begin{bmatrix} -1 & 0 & -2 & 4 \\ -0.5 & -1 & 1 & 1 \end{bmatrix}^\top, \ \underline{b}_1 = [1.2 \quad 0.8 \quad 2 \quad 3]^\top,$$

$$\mathbf{A}_2 = \begin{bmatrix} 0 & 1 & 1 & 0 & -1 & -1 & 1 & -1 \\ 1 & 1 & -1 & -1 & -1 & 1 & 0 & 0 \end{bmatrix}^\top,$$

$$\underline{b}_2 = [0.6 \quad 0.8 \quad 0.8 \quad 0.6 \quad 0.8 \quad 0.8 \quad 0.6 \quad 0.6]^\top$$

for different numbers of splittings.

We analyzed the behavior of the approximation error during progressive probability mass computation. The results are depicted in Figs. 5 and 6. In Fig. 6, it can be seen how the approximation error reduces for a growing number of splittings. As a baseline method, we used the ellipsoidal approximation approach proposed by van Hessem et. al. in [10]. The true probability mass was computed using stochastic sampling with 1 e 8 samples. A visual illustration of the approximation of the polytope $\mathcal{P}_1$ after different numbers of splittings is depicted in Fig. 7.

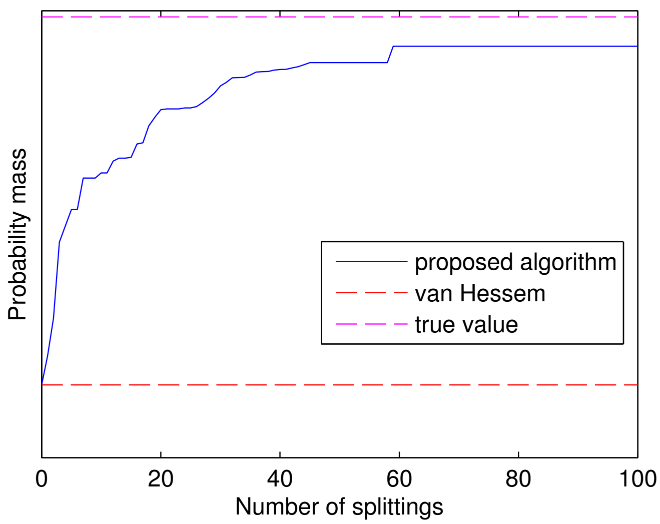

(a) Polytope $\mathcal{P}_1$.

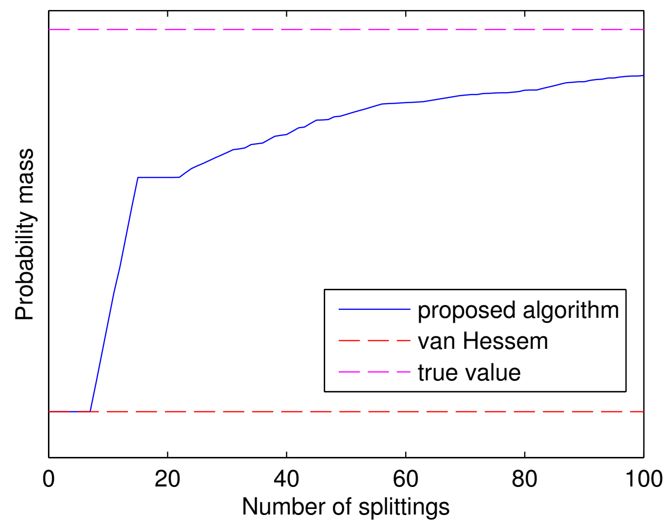

(b) Polytope $\mathcal{P}_2$.

Figure 6: Probability mass computation approximation error over number of splittings for $\mathcal{P}_1$ and $\mathcal{P}_2$.

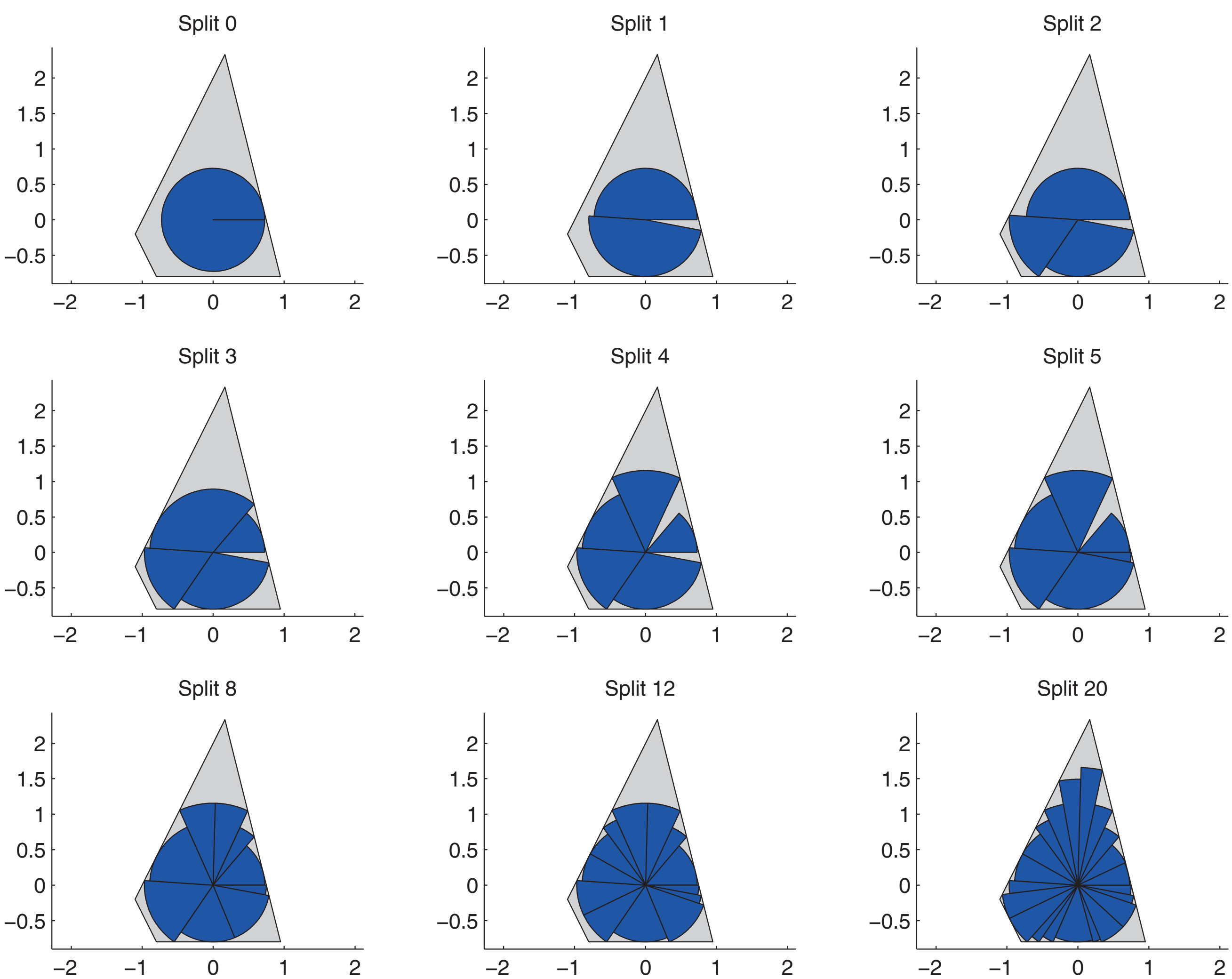

Figure 7: Demonstration of sector approximation of the polytope $\mathcal{P}_1$ after several splittings.

VI. Conclusion

In this paper, we presented a novel approach to (approximate) computation of the probability mass of a multivariate Gaussian over a polytopic domain. The proposed method relies on the approximation of the underlying domain, i.e., the polytope, in contrast to other algorithms that approximate the probability density itself. The main idea of our approach consists in conversion of the numerical integration into an optimization problem that progressively approximates the polytope from the inside using axis-aligned n-spherical sectors. The probability mass contained in these sectors can then be evaluated using a closed-form formula. As an intermediate result, we derived an algorithm for computation of the volume of the polytope using disjoint axis-aligned sectors.

Our future work will concentrate on the evaluation of the presented algorithm with regard to both approximation quality and speed compared to state-of-the-art methods such as MCMC. For this purpose, we will implement it efficiently in Matlab and C/C++.

Appendix A
Converting Spherical Coordinates into Cartesian

Given an n-dimensional vector $\underline{\xi}$ with

$$\underline{\xi} = [r \quad \phi_1 \quad \phi_2 \quad \dots \quad \phi_{n-1}] \ ,$$

in spherical coordinates, its representation in Cartesian coordinates

$$\underline{x} = [x_1 \quad x_2 \quad \dots \quad x_n]^\top$$

can be calculated according to

$$\begin{aligned} x_1 &= r\cos(\phi_1) \ , \\ x_2 &= r\sin(\phi_1)\cos(\phi_2) \ , \\ x_3 &= r\sin(\phi_1)\sin(\phi_2)\cos(\phi_3) \ , \\ &\vdots \\ x_{n-1} &= r\sin(\phi_1)\dots\sin(\phi_{n-2})\cos(\phi_{n-1}) \ , \\ x_n &= r\sin(\phi_1)\dots\sin(\phi_{n-2})\sin(\phi_{n-1}) \ . \end{aligned}$$

Appendix B
Proof of Theorem 1

The volume contained within the sector $\mathcal{S}_i$ is the solution of the integral

$$V_i = \int_0^R \int_0^{\delta_1} \dots \int_0^{\delta_{n-1}} \mathrm{d}V \ ,$$

where we exploited symmetry of the sphere defined by $\mathcal{S}_i$ by changing the angular integration interval from $[\phi_j; \phi_j + \delta_j]$ to $[0; \delta_j]$, $j = 1, \dots, n-1$. The volume element for an n-sphere is given by

$$\begin{aligned} \mathrm{d}V = & \, r^{n-1}\sin^{n-2}(\phi_1)\sin^{n-3}(\phi_2)\cdots\sin(\phi_{n-2}) \\ & \times \mathrm{d}r \ \mathrm{d}\phi_1 \ \mathrm{d}\phi_2 \ \cdots \ \mathrm{d}\phi_{n-2} \ \mathrm{d}\phi_{n-1} \ . \end{aligned}$$

Since the sectors are axis-aligned, integration w.r.t. every individual variable can be performed independently. Integration w.r.t. the radius yields

$$\int_0^R r^{n-1}\mathrm{d}r = \frac{1}{n}R^n \ .$$

For the integration w.r.t. $\phi_1, \dots, \phi_{n-2}$, we make use of the following recursion [17]

$$\int \sin^n(x)\mathrm{d}x = -\frac{1}{n}\sin^{n-1}(x)\cos(x) + \frac{n-1}{n}\int \sin^{n-2}(x)\mathrm{d}x \ .$$

By rewriting this recursion as a sum, we obtain the function $\gamma_n(\cdot)$ given in Theorem 2. Consequently, we obtain the following expression

$$\begin{aligned} &\int_0^{\delta_1}\int_0^{\delta_2}\cdots\int_0^{\delta_{n-2}} \sin^{n-2}(\phi_1)\sin^{n-3}(\phi_2)\cdots\sin(\phi_{n-2}) \\ &\quad \times \mathrm{d}\phi_1 \ \mathrm{d}\phi_2 \ \cdots \ \mathrm{d}\phi_{n-2} \\ &\quad = \int_0^{\delta_1}\sin^{n-2}(\phi_1)\mathrm{d}\phi_1 \ \int_0^{\delta_2}\sin^{n-3}(\phi_2)\mathrm{d}\phi_2 \ \dots \\ &\quad \times \int_0^{\delta_{n-2}}\sin(\phi_{n-2})\mathrm{d}\phi_{n-2} \\ &\quad = [\gamma_1(\delta_{n-2}) - \gamma_1(0)]\,[\gamma_2(\delta_{n-3}) - \gamma_2(0)]\cdots \\ &\quad \times [\gamma_{n-2}(\delta_1) - \gamma_{n-2}(0)] \\ &\quad = \prod_{i=1}^{n-2}[\gamma_i(\delta_{n-i-1}) - \gamma_i(0)] \end{aligned}$$

Finally, integration w.r.t. ϕ_{n-1} yields

$$\int_0^{\delta_{n-1}} \mathrm{d}\phi_{n-1} = \delta_{n-1} \ .$$

Combination of these intermediate results yields (4).

Acknowledgment

This work was supported by the German Research Foundation (DFG) within the Research Training Group RTG 1194 “Self-organizing Sensor-Actuator-Networks”.

References

[1] A. Prékopa, “The Use of Discrete Moment Bounds in Probabilistic Constrained Stochastic Programming Models,” *Annals of Operations Research*, vol. 85, pp. 21–38, 1999.

[2] A. Nemirovski and A. Shapiro, “Convex Approximations of Chance Constrained Programs,” *SIAM Journal of Optimization*, vol. 17, pp. 969–996, 2006.

[3] A. Nemirovski, “On Safe Tractable Approximations of Chance Constraints,” *European Journal of Operational Research*, vol. 219, no. 3, pp. 707 – 718, 2012.

[4] L. Blackmore, M. Ono, A. Bektassov, and B. C. Williams, “A Probabilistic Particle-control Approximation of Chance-constrained Stochastic Predictive Control,” *IEEE Transactions on Robotics*, vol. 26, no. 3, pp. 502–517, Jun. 2010.

[5] G. Calafiore and L. Fagiano, “Robust model predictive control via random convex programming,” in *Proceedings of the 50th IEEE Conference on Decision and Control and European Control Conference (CDC-ECC 2011)*, Dec 2011, pp. 1910–1915.

[6] ——, “Robust Model Predictive Control via Scenario Optimization,” *IEEE Transactions on Automatic Control*, vol. 58, no. 1, pp. 219–224, Jan 2013.

[7] N. Nomura, “Computation of Multivariate Normal Probabilities with Polar Coordinate Systems,” *Journal of Statistical Computation and Simulation*, vol. 84, no. 3, pp. 491–512, 2014.

[8] A. Genz and K.-S. Kwong, “Numerical Evaluation of Singular Multivariate Normal Distributions,” *Journal of Statistical Computation and Simulation*, vol. 68, pp. 1–21, 1999.

[9] J. P. Cunningham, P. Hennig, and S. Lacoste-Julien, “Gaussian Probabilities and Expectation Propagation,” *arXiv.org*, vol. stat/1111.6832, 2013.

[10] D. van Hessem and O. Bosgra, “Closed-loop Stochastic Dynamic Process Optimization under Input and State Constraints,” in *Proceedings of the 2002 American Control Conference (ACC 2002)*, 2002.

[11] ——, “A Conic Reformulation of Model Predictive Control including Bounded and Stochastic Disturbances under State and Input Constraints,” in *Proceedings of the 41st IEEE Conference on Decision and Control (CDC 2002)*, Dec 2002.

[12] “Sphere wireframe,” 2008, modified. [Online]. Available: http://commons.wikimedia.org

[13] L. Blackmore and M. Ono, “Convex Chance Constrained Predictive Control without Sampling,” *Proceedings of the AIAA Guidance, Navigation and Control Conference*, 2009.

[14] A. Nemirovski and A. Shapiro, “Scenario Approximations of Chance Constraints,” in *Probabilistic and Randomized Methods for Design under Uncertainty*, G. Calafiore and F. Dabbene, Eds. London: Springer, 2006.

[15] G. Calafiore and M. Campi, “Uncertain Convex Programs: Randomized Solutions and Confidence Levels,” *Mathematical Programming*, vol. 102, no. 1, pp. 25–46, 2005.

[16] ——, “Sampled Convex Programs and Probabilistically Robust Design.” in *Probabilistic and Randomized Methods for Design under Uncertainty*, G. Calafiore and F. Dabbene, Eds. London: Springer, 2006.

[17] M. Abramowitz and I. A. Stegun, Eds., *Handbook of Mathematical Functions with Formulas, Graphs, and Mathematical Tables*, 10th ed., ser. Applied Mathematics Series - 55. Washington, D.C.: U. S. Government Printing Office, 1972.